

Research Article

Entanglement Quantification of Correlated Photons Generated by Three-Level Laser with Parametric Amplifier and Coupled to a Two-Mode Vacuum Reservoir

Chimdessa Gashu , Ebisa Mosisa, and Tamirat Abebe 

Department of Physics, Jimma University, P.O. Box 378, Jimma, Ethiopia

Correspondence should be addressed to Tamirat Abebe; tam1704@gmail.com

Received 14 February 2020; Revised 1 April 2020; Accepted 22 April 2020; Published 18 May 2020

Academic Editor: Zine El Abiddine Fellah

Copyright © 2020 Chimdessa Gashu et al. This is an open access article distributed under the Creative Commons Attribution License, which permits unrestricted use, distribution, and reproduction in any medium, provided the original work is properly cited.

In this paper, the detailed inseparability criteria of entanglement quantification of correlated two-mode light generated by a three-level laser with a coherently driven parametric amplifier and coupled to a two-mode vacuum reservoir is thoroughly analyzed. Using the master equation, we obtain the stochastic differential equation and the correlation properties of the noise forces associated with the normal ordering. Next, we study the squeezing and the photon entanglement by considering different inseparability criteria. The various criteria of entanglement used in this paper show that the light generated by the quantum optical system is entangled and the amount of entanglement is amplified by introducing the parametric amplifier into the laser cavity and manipulating the linear gain coefficient.

1. Introduction

A three-level cascade laser has a great deal of interest over the years in connection with its potential as a source of the strong correlated photons exhibiting various nonclassical properties [1–6]. One of the possible mechanisms of producing this strong correlation is linked to atomic coherence that can be induced by preparing the atoms initially in a coherent superposition of the up and down levels [7, 8]. In this regard, three-level lasers can be defined as a two-photon quantum optical device that produces a strong correlated light with some nonclassical features such as squeezing and entanglement which are the subject of this paper. It turns out that the correlation induced by coupling the dipole forbidden transition, the up and down states of the three-level cascade atom, results in the generation of a strong continuous variable entanglement [9, 10]. Such atomic correlation is also called injected atomic coherence which occurs when the three-level atoms are prepared initially in a coherent superposition of the up and down states [10].

Quantum entanglement has been considered as the non-locality aspect of quantum correlations with no classical sim-

ilarity. This wonderful feature was investigated in the seminal paper of Einstein-Podolsky-Rosen (EPR) [11]. After that, Bell recognized that entanglement leads to experimentally testable deviations of quantum mechanics from classical physics [12]. Furthermore, with the advent of quantum information theory, entanglement was known as a resource for many applications such as quantum cryptography [13], quantum computation and communication [14], quantum dense coding [15], quantum teleportation [16], entanglement swapping [17], sensitive measurements [18], and quantum telecloning [19]. Hence, an interest of understanding entanglement creation and quantification has gained the attention of several authors [20–30].

Moreover, many schemes have been proposed to produce a strong entangled light from a three-level laser using different techniques theoretically [24–34]. Authors have studied the effect of a parametric amplifier on the quantum properties of light generated by the three-level laser [26, 28]. Alebachew has found that the parametric amplifier in the laser cavity increases the degree of entanglement [26]. This work has been confined to the case in which the steady state analysis is above the threshold condition. However, the solutions

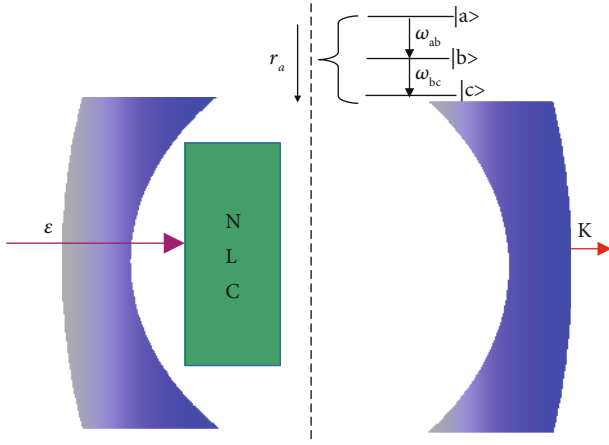


FIGURE 1: Schematic representation of nondegenerate three-level laser with a nonlinear crystal (NLC) and coupled to a two-mode vacuum reservoir. Here, ε , considered to be real and constant, is proportional to the amplitude of the pump mode that drives the NLC, r_a represents the rate at which the atoms are injected into the cavity, and κ is cavity damping constant, and it is assumed the same for both transitions.

to the cavity mode variables cannot be above the threshold condition of the steady state analysis [10, 30, 32]. Moreover, the entanglement quantification criteria have been limited to the Duan et al. criterion.

In this paper, the entanglement of the light produced by a nondegenerate three-level laser with nondegenerate parametric amplifier and coupled to vacuum reservoir is studied at or below the threshold condition resulting from the steady state solutions. Various criteria of entanglement quantification are used to study the entanglement of the two-mode light generated by the two-photon optical device in this paper. Moreover, the importance of the minus quadrature fluctuation in quantifying the two-mode entanglement is investigated in comparison with the other criteria. We consider a nondegenerate three-level laser in which the pump mode emerging from the parametric amplifier does not couple the up and down levels of the injected atoms. This could be realized by putting on the right side of the parametric amplifier a screen which absorbs the pump mode [35]. We carry out our analysis applying the pertinent master equation describing the dynamics of the optical device [36]. The solutions are presented for c -number cavity mode variables and correlation property of noise forces associated with normal ordering. Using the resulting solutions and steady state consideration, the mean photon number of the cross-correlation and separate cavity mode, quadrature squeezing, EPR variables, the smallest eigenvalue of the symplectic matrix, and Cauchy-Schwarz inequality of the cavity mode variables are determined.

The paper is organized as follows. In the second section, the Hamiltonian and the model are presented, the master equation describing the dynamics of the optical device is derived, and the solutions of the cavity mode variables are determined. In the last two sections, applying the solutions of the cavity mode variables, the quadrature squeezing and entanglement using various quantification criteria are investigated.

2. Hamiltonian and Master Equation

As it is clearly indicated in Figure 1, the top, intermediate, and bottom levels of a three-level atom are represented by $|a\rangle$, $|b\rangle$, and $|c\rangle$. We assume the transitions between levels $|a\rangle$ and $|b\rangle$ and between levels $|b\rangle$ and $|c\rangle$ to be dipole allowed, with direct transitions between levels $|a\rangle$ and $|c\rangle$ to be dipole forbidden. We consider the case for which the two cavity modes are at resonance with the two transitions $|a\rangle \rightarrow |b\rangle$ and $|b\rangle \rightarrow |c\rangle$ having transition frequencies ω_{ab} and ω_{bc} , respectively.

In the nondegenerate three-level laser, a pump mode photon of frequency $\omega = \omega_{ab} + \omega_{bc}$ directly interacts with the NLC to produce the signal-idler photon pairs having the same frequencies as the two cavity modes [25, 35, 36]. The interaction of three-level atoms with a nondegenerate parametric amplifier can be described by the Hamiltonian [30]:

$$\hat{H}_1 = i\varepsilon(\hat{a}^\dagger \hat{b}^\dagger - \hat{a} \hat{b}). \quad (1)$$

\hat{a} and \hat{b} are the annihilation operators for the two cavity modes. The master equation associated with this Hamiltonian has the following form [25, 30]:

$$\frac{d}{dt} \hat{\rho}(t) = \varepsilon(\hat{a}^\dagger \hat{b}^\dagger \hat{\rho} - \hat{\rho} \hat{a}^\dagger \hat{b}^\dagger - \hat{a} \hat{b} \hat{\rho} + \hat{\rho} \hat{a} \hat{b}), \quad (2)$$

where $\hat{\rho}$ is the density operator describing the mixed states.

In addition, the interaction of a nondegenerate three-level cascade atom with two-mode cavity radiation can be expressed in the interaction picture with the rotating-wave approximation (RWA) by the Hamiltonian of the form [30]

$$\hat{H}_I = ig[|a\rangle\langle b| \hat{a} - \hat{a}^\dagger |b\rangle\langle a| + |b\rangle\langle c| \hat{b} - \hat{b}^\dagger |c\rangle\langle b|], \quad (3)$$

where g is the coupling constant between the atom and cavity mode, and it is assumed the same for both transitions. In this paper, we suppose the state of a single three-level atom initially in

$$|\psi_A(0)\rangle = C_a|a\rangle + C_c|c\rangle, \quad (4)$$

and hence, the density operator of a single atom is

$$\hat{\rho}_A(0) = \rho_{aa}^{(0)}|a\rangle\langle a| + \rho_{ac}^{(0)}|a\rangle\langle c| + \rho_{ca}^{(0)}|c\rangle\langle a| + \rho_{cc}^{(0)}|c\rangle\langle c|, \quad (5)$$

where $\rho_{aa}^{(0)} = C_a^* C_a$, $\rho_{cc}^{(0)} = C_c^* C_c$, $\rho_{ac}^{(0)} = C_a C_c^*$, and $\rho_{ca}^{(0)} = C_c C_a^*$. Actually, this assumption corresponds to a situation in which the three-level atom is initially prepared in a coherent superposition of the up and down levels.

Thus, we apply the linear and adiabatic approximation schemes in the good cavity limit that the equation of the

density operator evolution for the cavity modes, in the absence of damping through the coupled mirror, has the form

$$\begin{aligned} \frac{d\hat{\rho}(t)}{dt} = & \frac{A\rho_{aa}^{(0)}}{2} [2\hat{a}^\dagger\hat{\rho}\hat{a} - \hat{a}\hat{a}^\dagger\hat{\rho} - \hat{\rho}\hat{a}\hat{a}^\dagger] \\ & + \frac{A\rho_{cc}^{(0)}}{2} [(2\hat{b}\hat{\rho}\hat{b}^\dagger - \hat{b}^\dagger\hat{b}\hat{\rho} - \hat{\rho}\hat{b}^\dagger\hat{b})] \\ & + \frac{1}{2}A\rho_{ac}^{(0)} [\hat{a}\hat{b}\hat{\rho} - \hat{a}^\dagger\hat{\rho}\hat{b}^\dagger + \hat{\rho}\hat{a}^\dagger\hat{b}^\dagger - \hat{b}\hat{\rho}\hat{a}] \\ & + \frac{1}{2}A\rho_{ca}^{(0)} [b^\dagger\hat{a}^\dagger\hat{\rho} - \hat{a}^\dagger\hat{\rho}\hat{b}^\dagger + \hat{\rho}\hat{a}\hat{b} - \hat{b}\hat{\rho}\hat{a}], \end{aligned} \quad (6)$$

where $A = 2g^2r_a/\gamma^2$ is the linear gain coefficient [10].

Next, we consider a system coupled with a two-mode vacuum reservoir. The density operator which is extracted from the vacuum reservoir by the partial trace operation is [10, 28, 30]

$$\begin{aligned} \frac{d\hat{\rho}}{dt} = & \frac{\kappa}{2} (2\hat{a}\hat{\rho}\hat{a}^\dagger - \hat{a}^\dagger\hat{a}\hat{\rho} - \hat{\rho}\hat{a}^\dagger\hat{a}) \\ & + \frac{\kappa}{2} (2\hat{b}\hat{\rho}\hat{b}^\dagger - \hat{b}^\dagger\hat{b}\hat{\rho} - \hat{\rho}\hat{b}^\dagger\hat{b}). \end{aligned} \quad (7)$$

Finally, using Equations (2), (6), and (7), the master equation for the system takes the form

$$\begin{aligned} \frac{d\hat{\rho}(t)}{dt} = & \varepsilon [\hat{\rho}\hat{a}\hat{b} - \hat{a}\hat{b}\hat{\rho} + \hat{a}^\dagger\hat{b}^\dagger\hat{\rho} - \hat{\rho}\hat{a}^\dagger\hat{b}^\dagger] \\ & + \frac{\kappa}{2} [2\hat{a}\hat{\rho}\hat{a}^\dagger - \hat{a}^\dagger\hat{a}\hat{\rho} - \hat{\rho}\hat{a}^\dagger\hat{a}] \\ & + \frac{1}{2}A\rho_{aa}^{(0)} [2\hat{a}^\dagger\hat{\rho}\hat{a} - \hat{a}\hat{a}^\dagger\hat{\rho} - \hat{\rho}\hat{a}\hat{a}^\dagger] \\ & + \frac{1}{2} (A\rho_{cc}^{(0)} + \kappa) [2\hat{b}\hat{\rho}\hat{b}^\dagger - \hat{b}^\dagger\hat{b}\hat{\rho} - \hat{\rho}\hat{b}^\dagger\hat{b}] \\ & + \frac{1}{2}A\rho_{ac}^{(0)} [\hat{a}\hat{b}\hat{\rho} - \hat{a}^\dagger\hat{\rho}\hat{b}^\dagger + \hat{\rho}\hat{a}^\dagger\hat{b}^\dagger - \hat{b}\hat{\rho}\hat{a}] \\ & + \frac{1}{2}A\rho_{ca}^{(0)} [b^\dagger\hat{a}^\dagger\hat{\rho} - \hat{a}^\dagger\hat{\rho}\hat{b}^\dagger + \hat{\rho}\hat{a}\hat{b} - \hat{b}\hat{\rho}\hat{a}]. \end{aligned} \quad (8)$$

The above master equation can be used to derive time variation for the expectation values of various system operators. The terms proportional to $\rho_{aa}^{(0)}$ and $\rho_{cc}^{(0)}$ describe the gain of cavity light for mode \hat{a} and the loss for mode \hat{b} , respectively. The terms proportional to $\rho_{ac}^{(0)}$ is related to the correlation of the generated radiation that indicates the existence of quantum features. These terms are responsible for the squeezing obtained in the cascade laser system. Furthermore, the terms proportional to κ describe the cavity mode damping due to its coupling with a two-mode vacuum reservoir via a single-port mirror.

On the basis of Equations (A.10) and (A.11), we can write

$$\frac{d}{dt}\alpha(t) = -\frac{\Gamma_1}{2}\alpha(t) + \frac{\Gamma_3}{2}\beta^*(t) + f_\alpha(t), \quad (9)$$

$$\frac{d}{dt}\beta^*(t) = -\frac{\Gamma_2}{2}\beta^*(t) - \frac{\Gamma_4}{2}\alpha(t) + f_\beta^*(t), \quad (10)$$

where $f_\alpha(t)$ and $f_\beta^*(t)$ are noise forces the properties of which remain to be determined, $\alpha(t)$ and $\beta(t)$ are the c -number variables corresponding to the cavity mode operators \hat{a} and \hat{b} , and

$$\Gamma_1 = \kappa - A\rho_{aa}(0), \quad (11)$$

$$\Gamma_2 = \kappa + A\rho_{cc}(0), \quad (12)$$

$$\Gamma_3 = 2\varepsilon - A\rho_{ac}(0), \quad (13)$$

$$\Gamma_4 = -(2\varepsilon + A\rho_{ac}(0)) \quad (14)$$

are the constant coefficients.

We now proceed to determine the properties of the noise forces. It is obvious that the expectation values of Equations (9) and (10) are identical to Equations (A.2) and (A.3) provided that

$$\langle f_\alpha(t) \rangle = \langle f_\beta(t) \rangle = 0. \quad (15)$$

Moreover, making use of Equations (9) and (10), one can verify that

$$\langle f_\alpha(t')f_\alpha(t) \rangle = 0, \quad (16)$$

$$\langle f_\beta(t)f_\beta(t') \rangle = \langle f_\alpha^*(t)f_\beta(t') \rangle = 0, \quad (17)$$

$$\langle f_\beta(t')f_\beta^*(t) \rangle = \langle f_\beta^*(t')f_\alpha(t) \rangle = 0, \quad (18)$$

$$\langle f_\alpha(t')f_\alpha^*(t) \rangle = A\rho_{aa}(0)\delta(t-t'), \quad (19)$$

$$\langle f_\beta(t')f_\alpha(t) \rangle = -\frac{\Gamma_4}{2}\delta(t-t'). \quad (20)$$

The results described by Equations (15)–(20) represent the correlation properties of the noise forces $f_\alpha(t)$ and $f_\beta(t)$ associated with the normal ordering. It proves to be useful to introduce a new parameter which relates the probabilities of the atom to be in the upper and lower levels. We define the parameter x such that

$$\rho_{aa}^{(0)} = \frac{1-x}{2}, \quad (21)$$

with $-1 < x < 1$. For three-level atoms initially in a coherent superposition of the up and down levels, we find applying Equation (21) that

$$\rho_{cc}^{(0)} = \frac{1+x}{2}, \quad (22)$$

and based on the relation $|\rho_{ac}^{(0)}|^2 = \rho_{aa}^{(0)}\rho_{cc}^{(0)}$, one can find easily

$$\rho_{ac}^{(0)} = \frac{1}{2}\sqrt{1-x^2}. \quad (23)$$

Hence, using Equations (11), (13), (21), (22), and (23) into Equations (9) and (10) results in

$$\frac{d}{dt}\alpha(t) = -\xi_+\alpha(t) - \eta_+\beta^*(t) + f_\alpha(t), \quad (24)$$

$$\frac{d}{dt}\beta^*(t) = -\xi_-\beta^*(t) - \eta_-\alpha(t) + f_\beta^*(t), \quad (25)$$

where

$$\begin{aligned} \xi_\pm &= \frac{1}{2} \left(\kappa + \frac{A}{2} [x \mp 1] \right), \\ \eta_\pm &= -\frac{1}{2} \left(2\varepsilon \mp \frac{A}{2} \sqrt{1-x^2} \right). \end{aligned} \quad (26)$$

We realize that Equations (24) and (25) are coupled differential equations. In order to solve these differential equations, we introduce a matrix equation of the form

$$\frac{d}{dt}Y(t) = -\frac{1}{2}RY(t) + F(t), \quad (27)$$

where

$$\begin{aligned} Y(t) &= \begin{pmatrix} \alpha(t) \\ \beta^*(t) \end{pmatrix}, \\ R &= \begin{pmatrix} \xi_+ & -\eta_+ \\ -\eta_- & \xi_- \end{pmatrix}, \\ F(t) &= \begin{pmatrix} f_\alpha(t) \\ f_\beta^*(t) \end{pmatrix}. \end{aligned} \quad (28)$$

Following the procedure described in Refs. [10, 36], we obtain

$$\begin{aligned} \alpha(t) &= A_+(t)\alpha(0) + B_+(t)\beta^*(0) + F_+(t) + W_+(t), \\ \beta(t) &= A_-(t)\beta(0) + B_-(t)\alpha^*(0) + F_-(t) + W_-(t), \end{aligned} \quad (29)$$

where

$$\begin{aligned} A_\pm(t) &= \frac{1}{2} \left[(1 \pm p)e^{-\lambda_- t} + (1 \mp p)e^{-\lambda_+ t} \right], \\ B_\pm(t) &= \frac{q_\pm}{2} \left[e^{-\lambda_+ t} - e^{-\lambda_- t} \right], \\ F_+(t) &= \frac{1}{2} \int_0^t \left[(1+p)e^{-\lambda_-(t-t')} + (1-p)e^{-\lambda_+(t-t')} \right] f_\alpha(t') dt', \\ F_-(t) &= \frac{1}{2} \int_0^t \left[(1-p)e^{-\lambda_-(t-t')} + (1+p)e^{-\lambda_+(t-t')} \right] f_\beta(t') dt', \\ W_+(t) &= \frac{q_+}{2} \int_0^t \left[e^{-\lambda_+(t-t')} - e^{-\lambda_-(t-t')} \right] f_\beta^*(t') dt', \end{aligned}$$

$$W_-(t) = \frac{q_-}{2} \int_0^t \left[e^{-\lambda_+(t-t')} - e^{-\lambda_-(t-t')} \right] f_\alpha^*(t') dt', \quad (30)$$

with

$$p = \frac{A}{\sqrt{16\varepsilon^2 + A^2x^2}}, \quad (31)$$

$$q_\pm = \frac{-4\varepsilon \pm A\sqrt{1-x^2}}{\sqrt{16\varepsilon^2 + A^2x^2}}, \quad (32)$$

$$\lambda_\pm = \frac{\kappa}{2} + \frac{1}{4} \left(Ax \pm \sqrt{16\varepsilon^2 + A^2x^2} \right). \quad (33)$$

At steady state, the system and the environment assume thermal equilibrium with each other. We observe that the equations of evolution of $\alpha(t)$ and $\beta(t)$ do not have well-behaved solutions for $\lambda_- < 0$. Hence, we note that the threshold condition for the system under consideration is attained when $\lambda_- = 0$. This condition yields by

$$\varepsilon_{\max} = \frac{1}{4} \sqrt{\kappa^2 + \kappa Ax}. \quad (34)$$

This provides the maximum possible value of the amplitude of parametric amplifier. The analysis is therefore confined to the case $\varepsilon \leq \varepsilon_{\max}$.

3. Quadrature Fluctuations

The quadrature fluctuations of the two-mode cavity radiation can be described by two quadrature operators:

$$\hat{c}_+ = (\hat{c}^\dagger + \hat{c}), \quad (35)$$

$$\hat{c}_- = i(\hat{c}^\dagger - \hat{c}), \quad (36)$$

where \hat{c} is the superposed cavity mode operator and given by

$$\hat{c} = \frac{1}{\sqrt{2}} (\hat{a} + \hat{b}). \quad (37)$$

We note that the operators described in Equations (35) and (36) are Hermitian and noncommuting. Based on this, the uncertainty relation between the quadrature operators can be written as

$$\Delta c_+^2 \Delta c_-^2 \geq 1. \quad (38)$$

Therefore, the two-mode cavity radiation is said to be in a squeezed state if either $\Delta c_+^2 < 1$ and $\Delta c_-^2 > 1$ or $\Delta c_+^2 > 1$ and $\Delta c_-^2 < 1$ such that $\Delta c_+ \Delta c_- \geq 1$ [35, 37, 38].

Thus, the fluctuations of the quadrature operators can be expressible as

$$\Delta c_\pm^2 = \langle \hat{c}_\pm^2 \rangle - \langle \hat{c}_\pm \rangle^2. \quad (39)$$

It is possible to express the variances of the quadrature operator Equations (35) and (36), in terms of the c -number variables associated with the normal ordering and supposing the cavity modes to be initially in a two-mode vacuum state, as

$$\begin{aligned} \Delta c_{\pm}^2 = & 1 + \langle \alpha^*(t)\alpha(t) \rangle + \langle \beta^*(t)\beta(t) \rangle \\ & + \langle \alpha^*(t)\beta(t) \rangle + \langle \alpha(t)\beta^*(t) \rangle \\ & \pm \left[\langle \alpha^*(t)\beta^*(t) \rangle + \langle \alpha(t)\beta(t) \rangle \right. \\ & \left. + \frac{1}{2} (\langle \alpha^2(t) \rangle + \langle \alpha^{*2}(t) \rangle + \langle \beta^{*2}(t) \rangle + \langle \beta^2(t) \rangle) \right]. \end{aligned} \quad (40)$$

In view of the fact that the noise force at time t does not affect the cavity mode variables at earlier times and taking the cavity modes to be initially in a vacuum state, it is also possible to verify, at a steady state, that

$$\langle \alpha^2 \rangle = \langle \beta^2 \rangle = \langle \alpha^* \beta \rangle = 0, \quad (41)$$

$$\begin{aligned} \langle \alpha^* \alpha \rangle = & \left[\frac{A(1-x)(1-p)^2}{16\lambda_+} + \frac{(A\sqrt{1-x^2} + 4\epsilon)q_+(1-p)}{16\lambda_+} \right] \\ & + \left[\frac{A(1-x)(1+p)^2}{16\lambda_-} \right] - \left[\frac{(A\sqrt{1-x^2} + 4\epsilon)q_+(1+p)}{16\lambda_-} \right] \\ & + \left[\frac{A(1-x)(1-p^2)}{4(\lambda_+ + \lambda_-)} + \frac{(A\sqrt{1-x^2} + 4\epsilon)q_+p}{4(\lambda_+ + \lambda_-)} \right], \end{aligned} \quad (42)$$

$$\begin{aligned} \langle \beta^* \beta \rangle = & \left[\frac{A(1-x)q_-^2}{16\lambda_+} + \frac{(A\sqrt{1-x^2} + 4\epsilon)q_-(1+p)}{16\lambda_+} \right] \\ & + \left[\frac{A(1-x)q_-^2}{16\lambda_-} \right] - \left[\frac{(A\sqrt{1-x^2} + 4\epsilon)q_-(1-p)}{16\lambda_-} \right] \\ & - \left[\frac{A(1-x)q_-^2}{4(\lambda_+ + \lambda_-)} + \frac{(A\sqrt{1-x^2} + 4\epsilon)q_-p}{4(\lambda_+ + \lambda_-)} \right], \end{aligned} \quad (43)$$

$$\begin{aligned} \langle \alpha \beta \rangle = & \left[\frac{A(1-x)q_-(1-p)}{8\lambda_+} \right] + \left[\frac{(A\sqrt{1-x^2} + 4\epsilon)(1-p^2 + q_-q_+)}{16\lambda_+} \right] \\ & - \left[\frac{A(1-x)q_-(1+p)}{16\lambda_-} \right] + \left[\frac{(A\sqrt{1-x^2} + 4\epsilon)(1-p^2 + q_-q_+)}{16\lambda_-} \right] \\ & + \left[\frac{A(1-x)q_-p}{4(\lambda_+ + \lambda_-)} + \frac{(A\sqrt{1-x^2} + 4\epsilon)(1+p^2 - q_-q_+)}{8(\lambda_+ + \lambda_-)} \right]. \end{aligned} \quad (44)$$

We realize that $\langle \alpha \beta \rangle$ is a real variable so that it can be set equal with its complex conjugate $\langle \alpha^* \beta^* \rangle$. Now, with

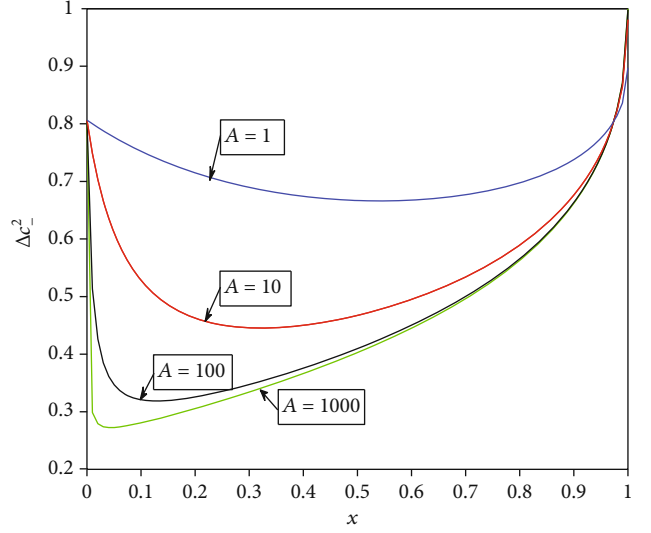


FIGURE 2: Quadrature variance Δc_{\pm}^2 versus x and for $\kappa = 0.5$, $\epsilon = 0.06$, and different values of the linear gain coefficient A .

the help of Equation (41) and using the steady state condition, Equation (40) can be obtained as

$$\Delta c_{\pm}^2 = 1 + \langle \alpha^* \alpha \rangle + \langle \beta^* \beta \rangle \pm 2\langle \alpha \beta \rangle. \quad (45)$$

Now, with the aid of Equations (31)–(33) together with (42)–(44), Equation (45) turns out to be

$$\begin{aligned} \Delta c_{\pm}^2 = & 1 + \left[A \left((1-x) \pm (A\sqrt{1-x^2} + 4\epsilon) \right) \pm 4\epsilon \right] \\ & \cdot \left[\frac{(\lambda_+ + \lambda_-)^2 + 4\lambda_+\lambda_-}{16\lambda_+\lambda_-(\lambda_+ + \lambda_-)} \right] + \left[A(1-x)(p^2 + q_-^2 \mp 2q_-p) \right. \\ & \left. - (A\sqrt{1-x^2} + 4\epsilon) [p(q_+ - q_-) \pm (p^2 - q_-q_+)] \right] \\ & \cdot \left[\frac{(\lambda_+ + \lambda_-)^2 - 4\lambda_+\lambda_-}{16\lambda_+\lambda_-(\lambda_+ + \lambda_-)} \right] + \left[A(1-x)(p \mp q_-) \right. \\ & \left. - (A\sqrt{1-x^2} + 4\epsilon)(q_+ + q_-) \right] \left[\frac{(\lambda_+ - \lambda_-)}{16\lambda_+\lambda_-} \right]. \end{aligned} \quad (46)$$

Equation (46) represents the variances of the cavity mode steady state for a nondegenerate three-level laser whose cavity contains a nondegenerate parametric amplifier and coupled to a two-mode vacuum reservoir.

We plot the intracavity quadrature variance of the two-mode light versus x for $\epsilon = 0.06$ and for different values of the linear gain coefficient in Figure 2. We easily see from this figure that the degree of squeezing increases with the linear gain coefficient. In addition, as the linear gain coefficient increases, the values of x at which the minimum value of the quadrature variance occurs tends to zero. We thus realize that better squeezing can be achieved by preparing the atoms initially in such a way that slightly more atoms are in the lower level than in the upper level and by increasing the

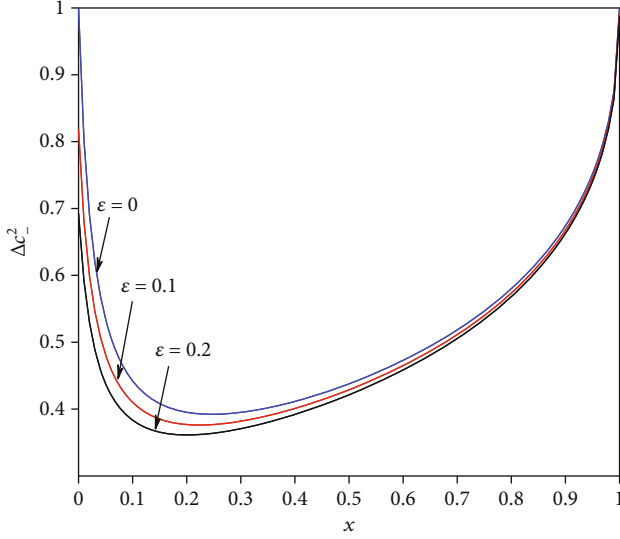


FIGURE 3: Quadrature variance Δc^2 versus x for $\kappa = 0.5$, $A = 50$, and different values of ε .

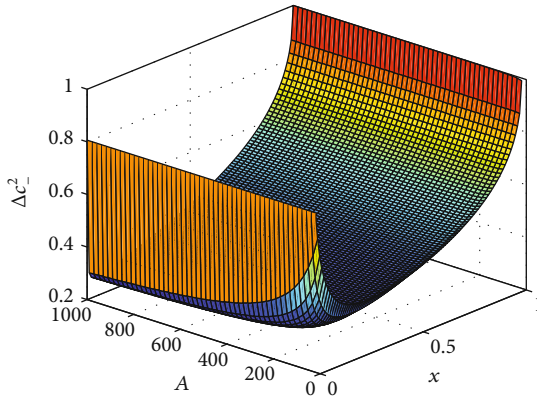


FIGURE 4: Quadrature variance Δc^2 versus the linear gain coefficient A and initial preparation of atoms x for $\kappa = 0.5$ and $\varepsilon = 0.06$.

linear gain coefficient. We also see that the degree of squeezing increases with the linear gain coefficient which is in a complete agreement with previous studies [7, 26, 28].

On the other hand, Figure 3 clearly shows that the presence of the parametric amplifier increases the intracavity degree of squeezing for small values of x . Thus, the presence of the parametric amplifier in the laser cavity leads to better squeezing. As indicated on these plots, when the parameter ε increases, the degree of squeezing also increases. Here, the maximum degree of squeezing for $A = 50$, $\kappa = 0.5$, and $\varepsilon = 0.2$ is found to be 62.7% which occurs at $x = 0.13$.

We easily see from Figure 4 the intracavity quadrature variance Δc^2 for the two-mode light versus A and x . This figure indicates that the system under consideration exhibits two-mode squeezing and the degree of squeezing increases with the parameter A which represents the linear gain coefficient. In addition, relatively better squeezing occurs for small values of x , when $\rho_{aa}^{(0)} < \rho_{cc}^{(0)}$. This would be related to the

atomic coherence transferred to the emitted photons which are more significant in this case.

4. Entanglement Quantification

Here, we study the degree of entanglement of the two-mode cavity light produced by a nondegenerate three-level cascade laser whose cavity contains a parametric amplifier. A pair of particles is taken to be entangled in quantum theory, if its states cannot be expressed as a product of the states of its individual constituents. The preparation and manipulation of these entangled states that have nonclassical and nonlocal properties lead to a better understanding of the basic quantum principles [39–41]. If the density operator for the combined state cannot be described as a combination of the product of density operators of the constituents,

$$\hat{\rho} \neq \sum_j P_j \hat{\rho}_j^{(1)} \otimes \hat{\rho}_j^{(2)}, \quad (47)$$

in which $P_j \geq 0$ and $\sum_j P_j = 1$ is set to ensure normalization of the combined density of state.

4.1. Duan-Giedke-Cirac-Zoller (DGCZ) Criterion. To study the entanglement of the quantum optical system, we consider the entanglement criterion set by Duan et al. [23]. Based on this criterion, a quantum state of the system is entangled if the sum of the variances of the two EPR-type operators \hat{u} and \hat{v} satisfies the condition [11]:

$$\Delta u^2 + \Delta v^2 < 2, \quad (48)$$

where

$$\begin{aligned} \hat{u} &= \hat{x}_a - \hat{x}_b, \\ \hat{v} &= \hat{p}_a + \hat{p}_b, \end{aligned} \quad (49)$$

in which $\hat{x}_a = (1/\sqrt{2})(\hat{a}^\dagger + \hat{a})$, $\hat{x}_b = (1/\sqrt{2})(\hat{b}^\dagger + \hat{b})$ and $\hat{p}_a = (i/\sqrt{2})(\hat{a}^\dagger - \hat{a})$, $\hat{p}_b = (i/\sqrt{2})(\hat{b}^\dagger - \hat{b})$ are the quadrature operators for modes \hat{a} and \hat{b} . The sum of the variances of \hat{u} and \hat{v} is easily found to be

$$\Delta u^2 + \Delta v^2 = 2[1 + \langle \alpha^* \alpha \rangle + \langle \beta^* \beta \rangle - 2\langle \alpha \beta \rangle]. \quad (50)$$

Comparing Equation (50) with Equation (45), we can obtain easily

$$\Delta u^2 + \Delta v^2 = 2\Delta c^2, \quad (51)$$

where Δc^2 is given in Equation (45). We see from this result that the degree of entanglement is directly proportional to the degree of squeezing of the two-mode light [7, 33, 34, 42]. In other words, the squeezing can be used to quantify and detect two-mode continuous variable entanglement. In this case, squeezing of the two-mode cavity light is used similar to the entanglement criterion proposed by Duan et al.

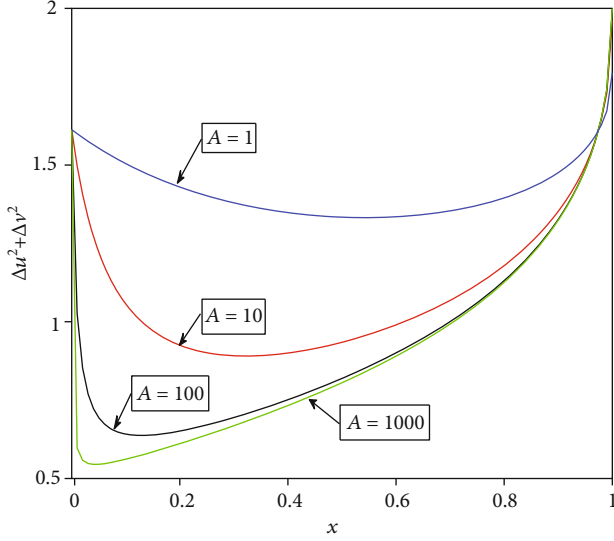


FIGURE 5: Duan et al. criterion $\Delta u^2 + \Delta v^2$ versus x for $\kappa = 0.5$, $\varepsilon = 0.06$, and different values of A .

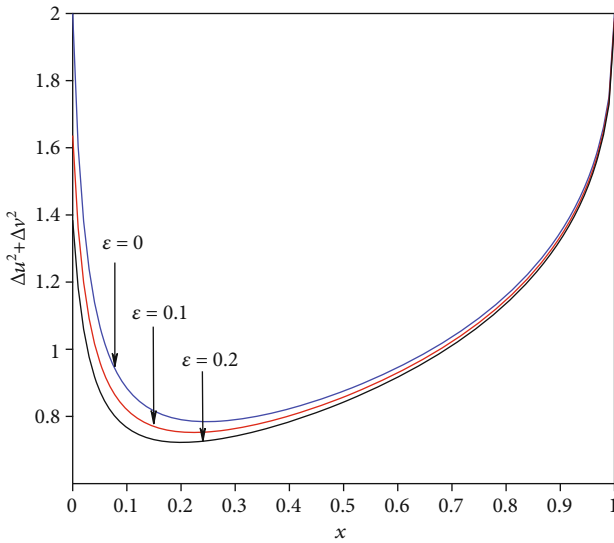


FIGURE 6: Duan et al. criterion $\Delta u^2 + \Delta v^2$ versus x for $\kappa = 0.5$, $A = 50$, and different values of ε .

It is also clearly indicated in Figure 5 that the cavity radiation is entangled for all considered parameters. It can be observed that the degree of entanglement increases by decreasing the values of the initial preparation of atoms. The maximum possible degree of entanglement in this case is found 73% for $A = 1000$ and $x = 0.04$. The introduction of the parametric amplifier is observed to improve the degree of entanglement for the minimum atomic coherence at which no entanglement was observed to occur in the earlier works [10].

Furthermore, it can be observed in Figure 6 that the degree entanglement of the cavity radiation is significantly enhanced with the linear gain coefficient. However, increasing more the linear gain coefficient does not lead to a significant change to

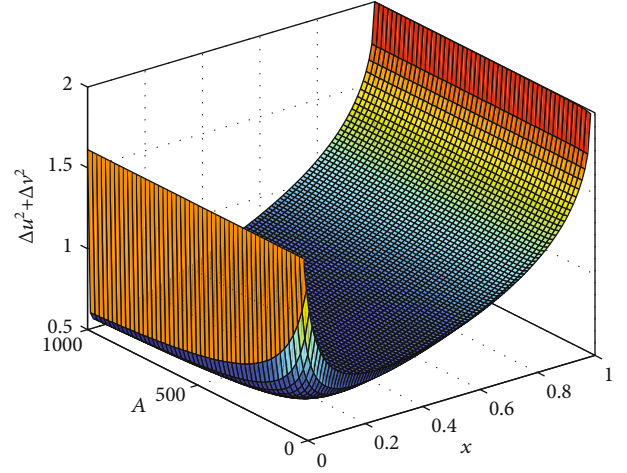


FIGURE 7: Duan et al. criterion $\Delta u^2 + \Delta v^2$ versus the linear gain coefficient A and initial preparation of atoms x for $\kappa = 0.5$ and $\varepsilon = 0.06$.

the maximum achievable degree of entanglement. A closer observation of this figure shows that the degree of entanglement at smaller values of the initial preparation of atoms is the same and solely attributed to the parametric amplifier inserted to the cavity. Moreover, stronger entangled light requires nearly an equal number of atoms at the top and bottom levels for larger values of the linear gain coefficient. On the other hand, the entanglement at the maximum initial preparation of atoms is smaller for a larger linear gain coefficient. This encourages the idea that the effect of the parametric amplifier is more prominent for smaller values of the linear gain coefficient and more number of atoms initially at the up level.

Furthermore, Figure 7 shows the degree of entanglement of the cavity radiation versus the linear gain coefficient A and the initial preparation of atoms x for $\kappa = 0.5$ and $\varepsilon = 0.06$. As we see from the figure, the degree of entanglement increases with the linear gain coefficient and for small values of x .

4.2. Logarithmic Negativity. Another criterion to study entanglement is the logarithmic negativity which is used for two-mode continuous variables based on the negativity of the partial transposition [29–31, 43]. The negative partial transpose must be parallel with respect to entanglement monotone in order to obtain the degree of entanglement. The logarithmic negativity is combined with negative partial transpose in another case where V represents the smallest eigenvalue of the symplectic matrix [29]:

$$V = \sqrt{\frac{\sigma - \sqrt{(\sigma^2 - 4 \det \Gamma)}}{2}}, \quad (52)$$

where the invariant and covariance matrices are, respectively, denoted as

$$\sigma = \det \Sigma_1 + \det \Sigma_2 - 2 \det \Sigma_{12}, \quad (53)$$

$$\Gamma = \begin{pmatrix} \Sigma_1 & \Sigma_{12} \\ \Sigma_{12}^T & \Sigma_2 \end{pmatrix}, \quad (54)$$

in which Σ_1 and Σ_2 are the covariance matrices describing each mode separately while Σ_{12} are the intermodal correlations. The elements of the matrix on Equation (54) are given by

$$\Gamma_{ij} = \frac{1}{2} \langle \widehat{X}_i \widehat{X}_j + \widehat{X}_j \widehat{X}_i \rangle - \langle \widehat{X}_i \rangle \langle \widehat{X}_j \rangle, \quad (55)$$

in which $i, j = 1, 2, 3, 4$. The quadrature operators are defined as $\widehat{X}_1 = \widehat{a} + \widehat{a}^\dagger$, $\widehat{X}_2 = i(\widehat{a}^\dagger - \widehat{a})$, $\widehat{X}_3 = \widehat{b} + \widehat{b}^\dagger$, and $\widehat{X}_4 = i(\widehat{b}^\dagger - \widehat{b})$. Now, we can extend the covariance matrix in terms of the c -number variables associated with the normal ordering noting that $\langle \alpha\beta \rangle = \langle \alpha^* \beta^* \rangle$ turns out to have the following form:

$$\Gamma = \begin{pmatrix} \Lambda & 0 & X & 0 \\ 0 & \Lambda & 0 & -X \\ X & 0 & \Delta & 0 \\ 0 & -X & 0 & \Delta \end{pmatrix}, \quad (56)$$

where $\Lambda = 2\langle \alpha^* \alpha \rangle + 1$, $\chi = 2\langle \alpha\beta \rangle$, and $\Delta = 2\langle \beta^* \beta \rangle + 1$ are c -number variables associated with the normal ordering. The logarithmic negativity for a two-mode state is defined as [29]

$$E_N = \max [0, -\log_2 V]. \quad (57)$$

The entanglement is achieved when E_N is positive within the region of the lowest eigenvalue of covariance matrix $V < 1$.

Next, using Equations (54) and (56), one can readily show that

$$\det \Sigma_1 = [2\langle \alpha^* \alpha \rangle + 1]^2, \quad (58)$$

$$\det \Sigma_2 = [2\langle \beta^* \beta \rangle + 1]^2, \quad (59)$$

$$\det \Sigma_{12}^T = \det \Sigma_{12} = -4\langle \alpha\beta \rangle^2. \quad (60)$$

The determinant of the matrix in Equation (56) is found as

$$\det \Gamma = [\Lambda\Delta - \chi^2]^2, \quad (61)$$

which, using Equations (58)–(60), reduces to the following form:

$$\det \Gamma = \left[\sqrt{\det \Sigma_1 \det \Sigma_2} - \sqrt{\det \Sigma_{12}^T \det \Sigma_{12}} \right]^2. \quad (62)$$

As it can be observed in Figure 8, the degree of entanglement increases for smaller values of the initial preparation of atoms but decreases for larger values. It can also be seen that larger values of the linear gain coefficient produce a strong entangled light in this figure. The maximum

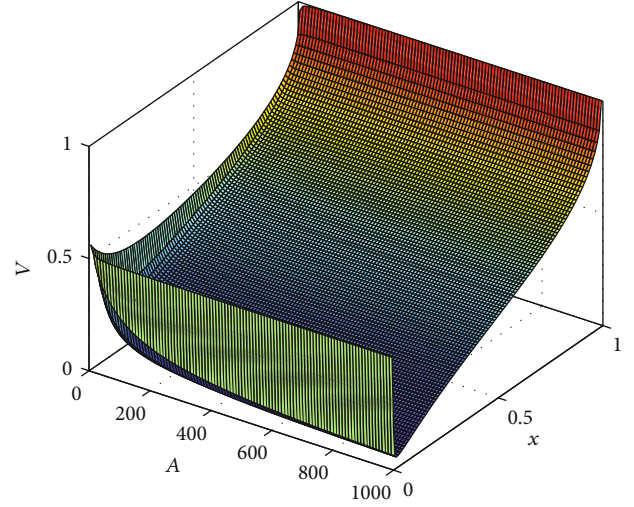


FIGURE 8: The smallest eigenvalue V of the two-mode cavity radiation versus the linear gain coefficient A and initial preparation of atoms x for $\kappa = 0.5$ and $\varepsilon = 0.06$.

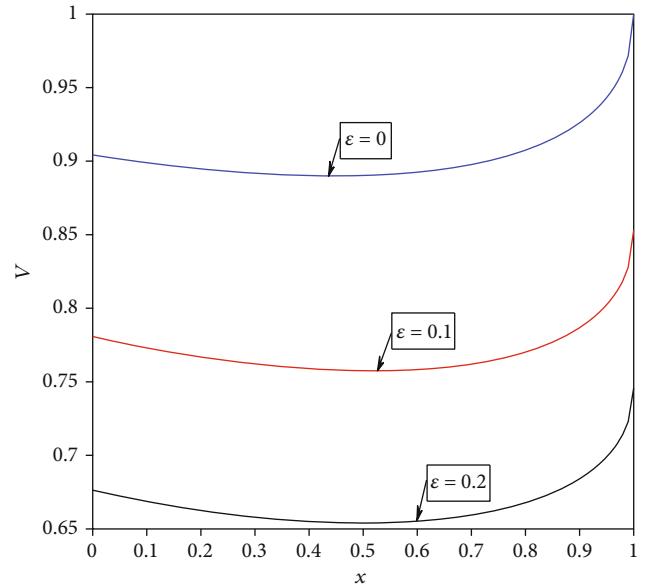


FIGURE 9: The smallest eigenvalue V of the two-mode cavity radiation versus x for $A = 0.5$, $\kappa = 0.9$, and different values of ε .

achievable degree of entangled light in this case is 96%, and it occurs for $A = 1000$ in $x = 0.0202$. This criterion also predicts the absence of entanglement for $x = 1$ no matter how we manipulate the rate of atomic injection in the absence of parametric amplifier as shown in Figure 8.

It is not difficult to see from Figure 9 that the parametric amplifier produces a significant change to the entanglement for a very small value of the linear gain coefficient regardless of how atoms are initially prepared. Exactly the same feature of the DGCZ criterion is observed in this figure except on the maximum achievable degree of entanglement.

Furthermore, it is clearly shown in Figure 10 that for the smaller rate of atomic injection, the maximum possible degree of entanglement prefers nearly an equal number of

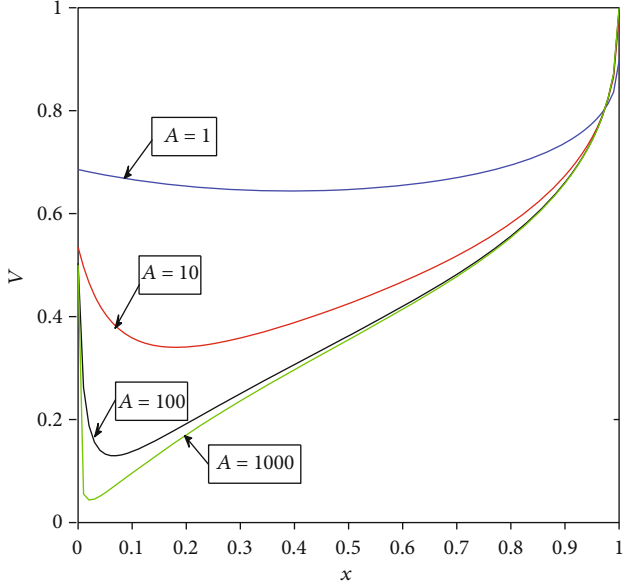


FIGURE 10: The smallest eigenvalue V of the two-mode cavity radiation versus x for $\kappa = 0.5$, $\varepsilon = 0.06$, and different values of A .

atoms initially prepared in the up and down levels. However, for the larger rate of atomic injection, a robust entangled light is produced when atoms are initially prepared nearly closer to the maximum atomic coherence. For example, this criterion predicts 96% of entanglement for $A = 1000$ and $x = 0.0202$.

On the other hand, Figure 11 compares the logarithmic negativity and quadrature fluctuation criteria in quantifying the entanglement. Even though the same pattern is observed in both cases, the logarithmic negativity criterion predicts a robust entangled light compared with the actually achievable degree in the DGCZ criterion. The degree of entanglement increases with the rate at which atoms are injected into the cavity, and it is found to be larger near the maximum atomic coherence in both cases. It is also worth noting that these approaches ascertain the entanglement when $x = 1$, which corresponds to the atoms initially prepared to be in the bottom level, which is solely attributed to the parametric amplifier.

4.3. Photon Antibunching. A photon antibunching phenomenon happens when the statistics of photons is scattered by passing time. It corresponds to fewer photon pairs detecting closer together in time. The correlation of scattered photons is studied via the second-order correlation function of photodetection with respect to time [10, 26, 30, 35, 36, 43]. Based on a photodetection experiment, for a coherent state, $g^{(2)}(\tau) = 1$ represents the highly correlated state [35, 36, 43]. In this state, the probability of joint detection coincides with the probabilities of independent detection [43].

On the other hand, $g^{(2)}(\tau) = 0$ when the time delay approaches infinity, $\tau \rightarrow \infty$, which means the joint probability of detecting the second photon decreases with time delay [35, 36, 43]. Thus, the situation $g^{(2)}(\tau) < g^{(2)}(0)$ is identified as photon bunching which means two photons tend to be detected simultaneously or after a short time delay [43]. If $g^{(2)}(\tau) > g^{(2)}(0)$, the joint probability of detecting the

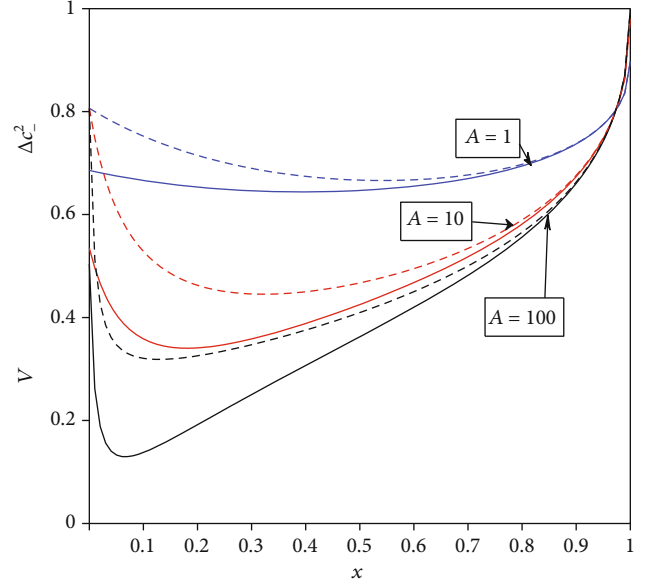


FIGURE 11: The minus quadrature variance Δc^2 (dashed curves) and the smallest eigenvalue V (solid curves) of the two-mode cavity radiation versus x for $\kappa = 0.5$, $\varepsilon = 0.06$, and different values of A .

second photon increases with time delay which is known as photon antibunching [35, 36, 43]. Here, $g^{(2)}(\tau) \rightarrow 1$ for $\tau \rightarrow \infty$ and $g^{(2)}(0) < 1$ implies the increased probability of detecting a second photon after a finite time delay, τ . This contradiction is the result of the quantum nature of light. Thus, photon antibunching is one of the methods to describe the entanglement. A field is said to be entangled if the inequality $g^{(2)}(\tau) > g^{(2)}(0)$ is satisfied [36, 43]. For the coherent state, $g^{(2)}(\tau) = 1$ represents a classical state. However, for a nonclassical state, we have $g^{(2)}(\tau) < 1$ which corresponds to the photon antibunching phenomenon occurrence. When $g^{(2)}(0) < 1$ and $g^{(2)}(\tau) > g^{(2)}(0)$, implying the presence of entanglement [43]. Unfortunately, it has been verified that $g^{(2)}(0) > 1$ for a nondegenerate three-level cascade laser while it is exhibiting the entanglement in some condition [4, 10, 26, 30, 35].

4.4. Hillery-Zubairy (HZ) Criterion. According to this criterion introduced by Hillery-Zubairy, for two modes of the electromagnetic field with \hat{a} and \hat{b} annihilation operators, the composite state is said to be entangled if condition

$$\left| \langle \hat{a}\hat{b} \rangle \right| > \sqrt{\langle \hat{n}_a \rangle \langle \hat{n}_b \rangle}, \quad (63)$$

is satisfied [37]. In this relation, \hat{n}_a and \hat{n}_b are the pertinent photon numbers corresponding to the involved modes. On the other hand, neglecting the interatomic interaction, the equal time photon number correlation for the two-mode cavity light can be expressed in terms of second-order correlation function in terms of c -number variables as [26]:

$$g^{(2)}(0) = 1 + \frac{\langle \alpha\beta \rangle^2}{\langle \alpha^* \alpha \rangle \langle \beta^* \beta \rangle}. \quad (64)$$

By considering the Hillery and Zubairy criterion, we can rewrite the above equation in the following form:

$$g^{(2)}(0) > 2. \quad (65)$$

It has been shown that the Hillery-Zubairy criterion is another equivalent entanglement criterion with Cauchy-Schwarz inequality when the interatomic interaction is neglected [30].

4.5. Violation of Cauchy-Schwarz Inequality (VCSI). We may also use the second-order correlation function to determine the entanglement of a two-mode cavity radiation [43]. A system of two-mode cavity radiation is said to be entangled if it violates the Cauchy-Schwarz inequality in the form

$$\langle \hat{a}^{\dagger 2} \hat{a}^2 \rangle \langle \hat{b}^{\dagger 2} \hat{b}^2 \rangle \geq \langle \hat{a}^{\dagger} \hat{b}^{\dagger} \hat{a} \hat{b} \rangle^2. \quad (66)$$

In this relation, it is possible to study the nonclassical photon number correlation at equal time using the following parameter [30]:

$$C_{ab} = \frac{|\langle \hat{a}^{\dagger} \hat{b}^{\dagger} \hat{a} \hat{b} \rangle|^2}{\langle \hat{a}^{\dagger 2} \hat{a}^2 \rangle \langle \hat{b}^{\dagger 2} \hat{b}^2 \rangle}. \quad (67)$$

Since the operators are already put in the normal order, the photon number correlation can be expressed, in terms of the c -number zero mean Gaussian variables α and β at steady state, as [30, 35]

$$\langle \alpha^* \alpha \beta^* \beta \rangle = \langle \alpha^* \alpha \rangle \langle \beta^* \beta \rangle + \langle \alpha \beta \rangle^2, \quad (68)$$

$$\langle \alpha^{*2} \alpha^2 \rangle = 2 \langle \alpha^* \alpha \rangle^2, \quad (69)$$

$$\langle \beta^{*2} \beta^2 \rangle = 2 \langle \beta^* \beta \rangle^2. \quad (70)$$

Now, applying Equations (68)–(70), we find that

$$C_{ab} = \frac{1}{4} \left[1 + \frac{\langle \alpha \beta \rangle^2}{\langle \alpha^* \alpha \rangle \langle \beta^* \beta \rangle} \right]^2. \quad (71)$$

It can be verified with the help of Equation (64) that

$$C_{ab} = \frac{1}{4} \left[g^{(2)}(0) \right]^2. \quad (72)$$

Using Equation (65), Equation (72) can be rewritten in the following form:

$$C_{ab} > 1. \quad (73)$$

Therefore, we plot C_{ab} versus the initial preparation of atoms and linear gain coefficient to study whether the cavity mode light is entangled or not. We also relate this approach with the minus quadrature variance to observe the variation of the approaches in quantifying the entanglement.

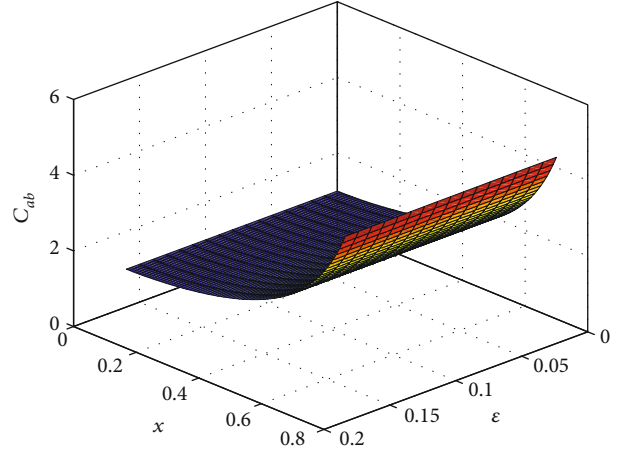


FIGURE 12: The steady state photon number correlation function C_{ab} of the two-mode cavity radiation versus the initial preparation of atoms x and amplitude of parametric amplifier ε for $A = 100$, $\kappa = 0.5$, and $\varepsilon = 0.06$.

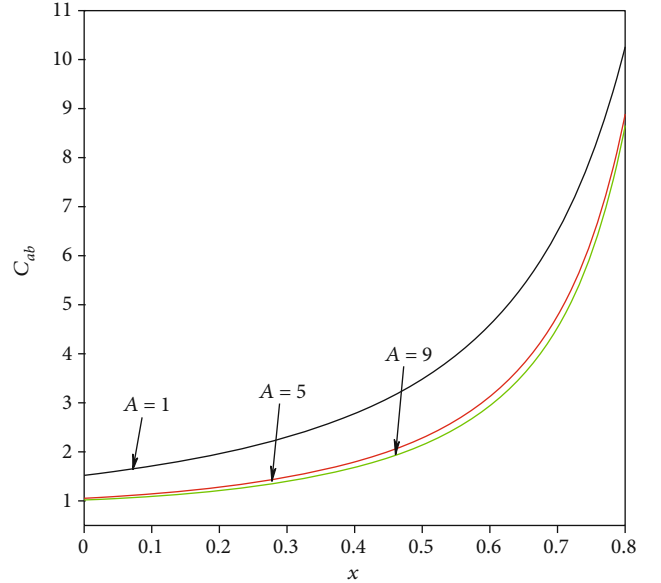


FIGURE 13: The steady state photon number correlation function C_{ab} of the two-mode cavity radiation versus x for $\kappa = 0.5$, $\varepsilon = 0.06$, and different values of A .

It is clearly shown in Figure 12 that the photon number correlation, C_{ab} , is greater than 1 for all considered values. This indicates that the nondegenerate three-level cascade laser with parametric amplifier is a source of entangled light, according to the Cauchy-Schwarz inequality and HZ criteria. It is also observed that the criterion does not include the case for which entanglement is weak when the procedure following from the logarithmic negativity and DGCZ criteria is applied.

Moreover, it can be observed in Figure 13 that C_{ab} increases with the decreasing rate of atomic injection. The same situation has been reported in terms of second-order correlation function for the case of the three-level laser that the degree of entanglement in this entanglement quantification approach is not necessarily directly proportional to the

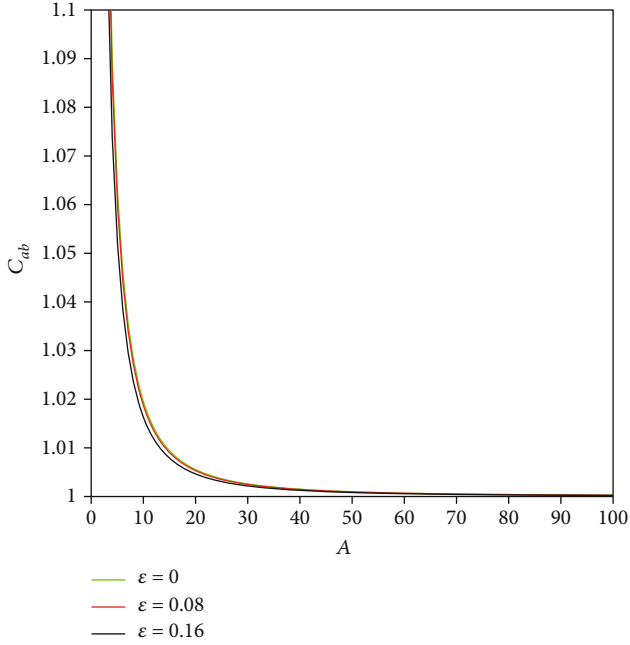


FIGURE 14: The steady state photon number correlation function C_{ab} of the two-mode cavity radiation versus x for $\kappa = 0.8$, $x = 0$, and different values of ϵ .

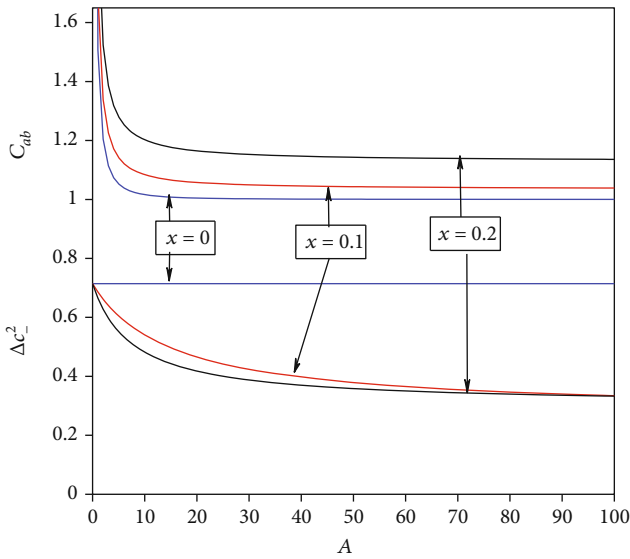


FIGURE 15: The steady state photon number correlation function C_{ab} of the two-mode cavity radiation versus x for $\kappa = 0.5$, $\epsilon = 0.06$, and different values of x .

extent to which this criterion is satisfied [30]. It is possible to realize that the Cauchy-Stewart inequality criterion can be important in predicting the presence of entanglement especially when the atomic coherence is close to maximum.

It is not difficult to observe in Figure 14 that C_{ab} increases with decreasing the rate of atomic injection and the amplitude of the parametric amplifier. It is also possible to realize from this approach that the effect of the parametric amplifier for larger values of the linear gain coefficient is insignificant. Therefore, the Cauchy-Schwarz inequality cri-

terion is encouraging entanglement quantification when the rate of atomic injection is larger and more photons are available in the cavity.

The plots in Figure 15 show the minus quadrature fluctuation, photon number correlation, and their relation in quantifying the entanglement. In actual sense, entanglement does not occur when atoms are initially prepared at the up and down levels. The observed degree of entanglement in this figure resulted from the parametric amplifier. It is found that further increment of the initial atomic preparation leads to larger value photon number correlation which does not necessary mean generation of a strong entangled light. It is inevitable that this situation does not account for the effect of larger values of the linear gain coefficient. We learned from the minus quadrature fluctuation that the initial preparation of atoms above the desired value decreases the entanglement. As one can see from the figure, the increment in the linear gain coefficient compensates for the suppressed degree of entanglement in ways of initially preparing atoms. This condition is not observed on the photon number correlation function. In general, the same pattern is observed by the two approaches when atoms are initially prepared equally or nearly equally at the top and bottom levels and for the considerable rate of atomic injection.

5. Conclusion

In this paper, different inseparability criteria have been used to quantify the entanglement of the two-mode cavity radiation of a nondegenerate three-level cascade laser whose cavity contains a nondegenerate parametric amplifier and coupled to a vacuum reservoir. The up and down levels of the three-level atoms are coupled by the initially prepared atoms in a coherent superposition. The degree of entanglement studied by logarithmic negativity and DGCZ criteria is greatly enhanced by increasing the rate of atomic injection when the atomic coherence is closer to its maximum value. In both cases, the weak entangled light is generated when all atoms are initially prepared in the lower energy state and a large number of atoms are constantly injected into the cavity regardless of the amplitude of the parametric amplifier. On the other hand, the important effect of the parametric amplifier occurs in both of these approaches for smaller values of the linear coefficient. In this situation, the two-mode light is found to be entangled even for the minimum and maximum atomic coherence which, respectively, corresponds to the absence and availability of more photons in the cavity.

Moreover, in DGCZ and logarithmic negativity criteria, increasing the linear gain coefficient compensates for the degraded degree of entanglement in ways of preparing the three-level atoms initially. Even though the Cauchy-Schwarz inequality detects the entanglement of the cavity radiation, it does not account for the effect of a large rate of atomic injection when the initial preparation of atoms is equal or close to the maximum atomic coherence. In this regard, the minus quadrature fluctuation and Cauchy-Schwarz inequality exhibit the same pattern of entanglement quantification for a considerable rate of atomic injection. On the other hand, the inequality does not include the case for which the

entangled light is weak when the procedure following from the logarithmic negativity and DGCZ criteria is applied. In contrast, the Cauchy-Schwarz inequality is found to be an encouraging approach specially when the rate of atomic injection is larger and more photons are available in the cavity.

In general, we found that the appeared behaviors of a nondegenerate three-level laser with and without a nondegenerate parametric amplifier are the same for the very large value of the linear gain coefficient (rate of atomic injection) except the detection of entanglement in the absence and presence of photons in the cavity.

Appendix

Stochastic Differential Equations

We now seek to obtain the stochastic differential equations associated with the normal ordering for the cavity mode variables. For this purpose, by making use of Equation (8) and the fact that

$$\frac{d}{dt}\langle\hat{A}\rangle = Tr\left(\frac{d\hat{\rho}(t)}{dt}\hat{A}\right), \quad (\text{A.1})$$

the time evolution of the expectation value of the cavity mode variables applying the cyclic property of the trace operation and taking into account the bosonic commutation relation is found to be

$$\frac{d}{dt}\langle\hat{a}\rangle = -\frac{\Gamma_1}{2}\langle\hat{a}\rangle + \frac{\Gamma_3}{2}\langle\hat{b}^\dagger\rangle, \quad (\text{A.2})$$

$$\frac{d}{dt}\langle\hat{b}\rangle = -\frac{\Gamma_2}{2}\langle\hat{b}\rangle + \frac{-\Gamma_4}{2}\langle\hat{a}^\dagger\rangle, \quad (\text{A.3})$$

$$\frac{d}{dt}\langle\hat{a}^2\rangle = -\Gamma_1\langle\hat{a}^2\rangle + \Gamma_3\langle\hat{b}^\dagger\hat{a}\rangle, \quad (\text{A.4})$$

$$\frac{d}{dt}\langle\hat{b}^2\rangle = -\Gamma_2\langle\hat{b}^2\rangle + \Gamma_4\langle\hat{a}^\dagger\hat{b}\rangle, \quad (\text{A.5})$$

$$\begin{aligned} \frac{d}{dt}\langle\hat{a}^\dagger\hat{a}\rangle &= -\Gamma_1\langle\hat{a}^\dagger\hat{a}\rangle + \frac{\Gamma_3}{2}\left[\langle\hat{a}^\dagger\hat{b}^\dagger\rangle + \langle\hat{a}\hat{b}\rangle\right] \\ &+ A\rho_{aa}(0), \end{aligned} \quad (\text{A.6})$$

$$\frac{d}{dt}\langle\hat{b}^\dagger\hat{b}\rangle = -\Gamma_2\langle\hat{b}^\dagger\hat{b}\rangle + \frac{\Gamma_4}{2}\left[\langle\hat{b}^\dagger\hat{a}^\dagger\rangle + \langle\hat{a}\hat{b}\rangle\right], \quad (\text{A.7})$$

$$\begin{aligned} \frac{d}{dt}\langle\hat{a}^\dagger\hat{b}\rangle &= -\frac{1}{2}(\Gamma_1 + \Gamma_2)\langle\hat{a}^\dagger\hat{b}\rangle + \frac{\Gamma_4}{2}\langle\hat{a}^{\dagger 2}\rangle \\ &+ \frac{\Gamma_3}{2}\langle\hat{b}^{\dagger 2}\rangle, \end{aligned} \quad (\text{A.8})$$

$$\begin{aligned} \frac{d}{dt}\langle\hat{a}\hat{b}\rangle &= -\frac{1}{2}(\Gamma_1 + \Gamma_2)\langle\hat{a}\hat{b}\rangle + \frac{\Gamma_4}{2}\langle\hat{a}^\dagger\hat{a}\rangle \\ &+ \frac{\Gamma_3}{2}\langle\hat{b}^\dagger\hat{b}\rangle + \frac{\Gamma_4}{2}. \end{aligned} \quad (\text{A.9})$$

We note that the operators in the above equations are in the normal order. The c -number equations corresponding to Equations (A.2)–(A.9) are

$$\frac{d}{dt}\langle\alpha(t)\rangle = -\frac{\Gamma_1}{2}\langle\alpha(t)\rangle + \frac{\Gamma_3}{2}\langle\beta^*(t)\rangle, \quad (\text{A.10})$$

$$\frac{d}{dt}\langle\beta(t)\rangle = -\frac{\Gamma_2}{2}\langle\beta(t)\rangle + \frac{-\Gamma_4}{2}\langle\alpha^*(t)\rangle, \quad (\text{A.11})$$

$$\frac{d}{dt}\langle\alpha^2(t)\rangle = -\Gamma_1\langle\alpha^2(t)\rangle + \Gamma_3\langle\beta^*(t)\alpha(t)\rangle, \quad (\text{A.12})$$

$$\frac{d}{dt}\langle\beta^2(t)\rangle = -\Gamma_2\langle\beta^2(t)\rangle + \Gamma_4\langle\alpha^*(t)\beta(t)\rangle, \quad (\text{A.13})$$

$$\begin{aligned} \frac{d}{dt}\langle\alpha^*(t)\alpha(t)\rangle &= -\Gamma_1\langle\alpha^*(t)\alpha(t)\rangle + \frac{\Gamma_3}{2}[\langle\alpha^*(t)\beta^*(t)\rangle \\ &+ \langle\alpha(t)\beta(t)\rangle] + A\rho_{aa}(0), \end{aligned} \quad (\text{A.14})$$

$$\begin{aligned} \frac{d}{dt}\langle\beta^*(t)\beta(t)\rangle &= -\Gamma_2\langle\beta^*(t)\beta(t)\rangle + \frac{\Gamma_4}{2}[\langle\beta^*(t)\alpha^*(t)\rangle \\ &+ \langle\alpha(t)\beta(t)\rangle], \end{aligned} \quad (\text{A.15})$$

$$\begin{aligned} \frac{d}{dt}\langle\alpha^*(t)\beta(t)\rangle &= -\frac{1}{2}(\Gamma_1 + \Gamma_2)\langle\alpha^*(t)\beta(t)\rangle \\ &+ \frac{\Gamma_4}{2}\langle\alpha^{*2}(t)\rangle + \frac{\Gamma_3}{2}\langle\beta^{*2}(t)\rangle, \end{aligned} \quad (\text{A.16})$$

$$\begin{aligned} \frac{d}{dt}\langle\alpha(t)\beta(t)\rangle &= -\frac{1}{2}(\Gamma_1 + \Gamma_2)\langle\alpha(t)\beta(t)\rangle + \frac{\Gamma_4}{2}\langle\alpha^*(t)\alpha(t)\rangle \\ &+ \frac{\Gamma_3}{2}\langle\beta^*(t)\beta(t)\rangle + \frac{\Gamma_4}{2}. \end{aligned} \quad (\text{A.17})$$

Data Availability

The data is included in the manuscript.

Conflicts of Interest

The authors declare that there is no conflict of interest regarding the publication of this paper.

Acknowledgments

It is our pleasure to thank Jimma University, college of natural sciences research and postgraduate coordination office, for all they did for us, their help, encouragement, and financial support during our research. This research is funded by Jimma University, college of natural sciences research and postgraduate coordination office.

References

- [1] C. W. Gardiner, "Inhibition of atomic phase decays by squeezed light: a direct effect of squeezing," *Physical Review Letters*, vol. 56, no. 18, pp. 1917–1920, 1986.
- [2] C. J. Villas-Boas and M. H. Y. Moussa, "One-step generation of high-quality squeezed and EPR states in cavity QED," *The European Physical Journal D - Atomic, Molecular, Optical and Plasma Physics*, vol. 32, no. 1, pp. 147–151, 2005.
- [3] S. Qamar, S. Qamar, and M. S. Zubairy, "Effect of phase fluctuations on entanglement generation in a correlated emission

- laser with injected coherence,” *Optics Communication*, vol. 283, no. 5, pp. 781–785, 2010.
- [4] S. Tesfa, “Effect of dephasing on quantum features of the cavity radiation of an externally pumped correlated emission laser,” *Physical Review A*, vol. 79, no. 6, article 063815, 2009.
 - [5] N. A. Ansari, J. Gea-Banacloche, and M. S. Zubairy, “Phase-sensitive amplification in a three-level atomic system,” *Physical Review A*, vol. 41, no. 9, pp. 5179–5186, 1990.
 - [6] H. Xiong, M. O. Scully, and M. S. Zubairy, “Correlated Spontaneous Emission Laser as an Entanglement Amplifier,” *Physical Review Letters*, vol. 94, no. 2, article 023601, 2005.
 - [7] E. Alebachew, “Enhanced squeezing and entanglement in a non-degenerate three-level cascade laser with injected squeezed light,” *Optics Communication*, vol. 280, no. 1, pp. 133–141, 2007.
 - [8] S. Qamar, M. Al-Amri, and M. S. Zubairy, “Entanglement in a bright light source via Raman-driven coherence,” *Physical Review A*, vol. 79, no. 1, article 013831, 2009.
 - [9] M. Kiffner, M. S. Zubairy, J. Evers, and C. H. Keitel, “Two-mode single-atom laser as a source of entangled light,” *Physical Review A*, vol. 75, no. 3, article 033816, 2007.
 - [10] S. Tesfa, “Entanglement amplification in a nondegenerate three-level cascade laser,” *Physical Review A*, vol. 74, no. 4, article 043816, 2006.
 - [11] A. Einstein, B. Podolsky, and R. Rosen, “Can quantum-mechanical description of physical reality be considered complete?,” *Physics Review*, vol. 47, no. 10, pp. 777–780, 1935.
 - [12] J. S. Bell, “On the Einstein Podolsky Rosen paradox,” *Physics*, vol. 1, no. 3, pp. 195–200, 1964.
 - [13] T. Jennewein, C. Simon, G. Weihs, H. Weinfurter, and A. Zeilinger, “Quantum cryptography with entangled photons,” *Physical Review Letters*, vol. 84, no. 20, pp. 4729–4732, 2000.
 - [14] C. H. Bennett and D. P. DiVincenzo, “Quantum information and computation,” *Nature*, vol. 404, no. 6775, pp. 247–255, 2000.
 - [15] S. Barzanjeh, S. Pirandola, and C. Weedbrook, “Continuous-variable dense coding by optomechanical cavities,” *Physical Review A*, vol. 88, no. 4, article 042331, 2013.
 - [16] N. Ganguly, S. Adhikari, A. S. Majumdar, and J. Chatterjee, “Entanglement witness operator for quantum teleportation,” *Physical Review Letters*, vol. 107, no. 27, article 270501, 2011.
 - [17] C. Branciard, N. Brunner, H. Buhrman et al., “Classical Simulation of Entanglement Swapping with Bounded Communication,” *Physical Review Letters*, vol. 109, no. 10, article 100401, 2012.
 - [18] T. Kitagawa, A. Aspect, M. Greiner, and E. Demler, “Phase-sensitive measurements of order parameters for ultracold atoms through two-particle interferometry,” *Physical Review Letters*, vol. 106, no. 11, article 115302, 2011.
 - [19] S. Koike, H. Takahashi, H. Yonezawa et al., “Demonstration of quantum telecloning of optical coherent states,” *Physical Review Letters*, vol. 96, no. 6, article 060504, 2006.
 - [20] R. T. Thew and W. J. Munro, “Entanglement manipulation and concentration,” *Physical Review A*, vol. 63, article 030302(R), 2001.
 - [21] K. Thapliyal, A. Pathak, B. Sen, and J. Peřina, “Higher-order nonclassicalities in a codirectional nonlinear optical coupler: Quantum entanglement, squeezing, and antibunching,” *Physical Review A*, vol. 90, no. 1, article 013808, 2014.
 - [22] J. Naikoo, K. Thapliyal, A. Pathak, and S. Banerjee, “Probing nonclassicality in an optically driven cavity with two atomic ensembles,” *Physical Review A*, vol. 97, no. 6, article 063840, 2018.
 - [23] L. M. Duan, G. Giedke, J. I. Cirac, and P. Zoller, “Inseparability criterion for continuous variable systems,” *Physical Review Letters*, vol. 84, no. 12, pp. 2722–2725, 2000.
 - [24] N. Lu, F.-X. Zhao, and J. Bergou, “Nonlinear theory of a two-photon correlated-spontaneous-emission laser: a coherently pumped two-level-two-photon laser,” *Physical Review A*, vol. 39, no. 10, pp. 5189–5208, 1989.
 - [25] B. Daniel and K. Fesseha, “The propagator formulation of the degenerate parametric oscillator,” *Optics Communication*, vol. 151, no. 4-6, pp. 384–394, 1998.
 - [26] E. Alebachew, “Continuous-variable entanglement in a nondegenerate three-level laser with a parametric oscillator,” *Physical Review A*, vol. 76, no. 2, article 023808, 2007.
 - [27] Y. H. Ma, Q. X. Mu, G. H. Yang, and L. Zhou, “Enhanced continuous-variable entanglement by a self-phase-locked type-II optical parameter oscillator with feedback loops,” *Journal of Physics B: Atomic, Molecular and Optical Physics*, vol. 41, no. 21, article 215502, 2008.
 - [28] T. Abebe, “Enhancement of squeezing and entanglement in a non-degenerate three-level cascade laser with coherently driven cavity,” *Ukrainian Journal of Physics*, vol. 63, no. 8, p. 733, 2018.
 - [29] G. Vidal and R. F. Werner, “Computable measure of entanglement,” *Physical Review A*, vol. 65, no. 3, article 032314, 2002.
 - [30] S. Tesfa, “A comparative study of entanglement amplification in a nondegenerate three-level cascade laser employing various inseparability criteria,” *Journal of Physics B: Atomic, Molecular and Optical Physics*, vol. 42, no. 21, article 215506, 2009.
 - [31] G. Adesso, A. Serafini, and F. Illuminati, “Extremal entanglement and mixedness in continuous variable systems,” *Physical Review A*, vol. 70, no. 2, article 022318, 2004.
 - [32] S. Tesfa, “Role of phase fluctuation and dephasing in the enhancing continuous variable entanglement of a two-photon coherent beat laser,” *Chinese Physics B*, vol. 21, no. 1, article 014204, 2012.
 - [33] T. Abebe, “The quantum analysis of nondegenerate three-level laser with spontaneous emission and noiseless vacuum reservoir,” *Ukrainian Journal of Physics*, vol. 63, no. 11, p. 969, 2018.
 - [34] T. Abebe, “Coherently driven nondegenerate three-level laser with noiseless vacuum reservoir,” *Bulgarian Journal of Physics*, vol. 45, no. 4, pp. 357–373, 2018.
 - [35] F. Kassahun, *Fundamental of Quantum Optics*, Lulu, Raleigh, NC, USA, 2008.
 - [36] M. Fox, *Quantum Optics: An Introduction*, Oxford University Press, Oxford, 2006.
 - [37] M. Hillery and M. S. Zubairy, “Entanglement conditions for two-mode states,” *Physical Review Letters*, vol. 96, no. 5, article 050503, 2006.
 - [38] G. J. Milburn and D. F. Walls, “Squeezed states and intensity fluctuations in degenerate parametric oscillation,” *Physical Review A*, vol. 27, no. 1, pp. 392–394, 1983.
 - [39] A. Karimi and M. K. Tavassoly, “Generation of entangled squeezed states: their entanglement and quantum polarization,” *Laser Physics*, vol. 25, no. 11, article 115201, 2015.
 - [40] A. Karimi and M. K. Tavassoly, “Generation of entangled coherent-squeezed states: their entanglement and nonclassical

- properties,” *Quantum Information Processing*, vol. 15, no. 4, pp. 1513–1527, 2016.
- [41] A. Karimi, “Two-mode photon-added entangled coherent-squeezed states: their entanglement and nonclassical properties,” *Applied Physics B: Lasers and Optics*, vol. 123, no. 6, p. 181, 2017.
- [42] R. J. Glauber, “Coherent and Incoherent States of the Radiation Field,” *Physics Review*, vol. 131, no. 6, pp. 2766–2788, 1963.
- [43] A. Sumairi, S. N. Hazmin, and C. R. Ooi, “Quantum entanglement criteria,” *Journal of Modern Optics*, vol. 60, no. 7, pp. 589–597, 2013.